A TEMPORAL FREQUENCY DESCRIPTION OF THE SPATIAL CORRELATION BETWEEN VOXELS IN FMRI DUE TO SPATIAL PROCESSING

by

Mary C. Kociuba

A Thesis Submitted to the Faculty of the Graduate School,
Marquette University,
in Partial Fulfillment of the Requirements
for the Degree of Master of Science

Milwaukee, Wisconsin

May 2013

ABSTRACT
A TEMPORAL FREQUENCY DESCRIPTION OF THE SPATIAL CORRELATION
BETWEEN VOXELS IN FMRI DUE
TO SPATIAL PROCESSING

Mary C. Kociuba

Marquette University, 2013

To correct the noise inherent within an acquired signal in fMRI and identify true biological spatiotemporal correlations, spatial and temporal filters are applied during the time series data processing. It is well known that spatial preprocessing induces correlation between voxels; applying a low pass spatial filter produces a smoother image, yet artificially increases the correlations between neighboring neural regions. The exact theoretical statistical relationships for the spatial covariance and spatial correlation matrices can be represented as a linear combination of second order voxel temporal frequencies. Developing this framework provides a means for quantifying the consequences of reconstruction and processing operations on the voxel temporal frequency spectrums, through identifying the temporal frequency bands that contribute significantly to induced correlations of no biological origin.

ACKNOWLEDGEMENTS

Mary C. Kociuba

I would like to give my sincere gratitude to Dr. Rowe, my advisor, for his time and support throughout the development of this project and furthering my understanding in the field of fMRI. I would also like to thank Iain Bruce, Muge Karaman, Yuning Chen, and Chaitan Parikh for their contributions in our research discussion sessions, and sharing their knowledge and resources in the field.

TABLE OF CONTENTS

I. INTRODUCTION

Functional magnetic resonance imaging (fMRI) is a noninvasive imaging method for observing activity in the brain. Brain activity is commonly detected by observing fluctuations in the blood oxygenation level dependent (BOLD) signal over time. As neural activity increases, the flow of diamagnetic oxygen-rich blood increases in the active region of the brain, resulting in decreased magnetic susceptibility of the blood, which is reflected in a higher measured signal in the region [Ogawa, 1990]. To observe these changes over time, a time series of images of the brain is reconstructed from the acquired signal. In an effort to reduce noise inherent within the signal, from sources such as subject movement and physiological BOLD fluctuations, various spatial and temporal processing operations are applied to the data. However, temporal and spatial processing operations applied to the data will introduce artificial neural correlations of no biological origin. To correctly identify the connectivity in the brain that is of true biological origin, the statistical spatial and temporal relationships within the data must be modeled accurately, such that the impact of the spatiotemporal processing operations can be accounted for when interpreting processed data.

Spatial and temporal processing operators are typically applied to the acquired and reconstructed data to reduce the effects of noise. For example, low pass filters are commonly applied to the data, to remove the high frequency noise associated with cardiac and respiratory oxygenation fluctuations that are acquired with the measured signal. Applying a low pass filter produces a smoother image, yet

artificially increases the correlations between neighboring regions. Previous studies verified that artificial spatial correlations are induced as a result of spatial reconstruction operators [Nencka, 2009], or parallel image reconstruction methods [Bruce, 2011] utilized during fMRI image processing. Recent studies [Davey, 2013] have investigated the degree to which filtering induces spatial correlations in resting state data functional connectivity MRI (fcMRI) data. Reconstructed images consist of biological, as well as artificially induced spatial correlations. In a fcMRI study, Biswal discovered that neural spatial correlations exist during the resting state between nonadjacent regions of the brain. During a resting state (non-task state), subjects exhibit synchronous low frequency (<0.08 Hz) physiological BOLD fluctuations at correlated regions. The regions correlated during the resting state also exhibit spatial task activated correlations, suggesting resting state functional connectivity is related to task activated correlated regions [Biswal, 1995]. In addition to connectivity observed within a single slice, functional connectivity correlations exist across the entire brain [Lowe, 1998].

The broader impact of this study will aid in the advancement of the understanding of brain activity associated with neurological disorders including degenerative diseases, development disorders, and mental health disorders. Studies show that patient populations with a specific neurological disorder exhibit similar functional connectivity. In fact, Alzheimer's disease, a degenerative neurological disease, patients display abnormal functionality in the hippocampus region of the brain years before the onset of the disease [Li, 2001]. Classifying a disease specific neurological biomarker identified with fMRI provides a noninvasive method to

monitor and detect the progression of neurological disease or benefit of prescribed therapies through observing connectivity in the brain during the course of a disease.

II. RESEARCH STATEMENT

Reconstructed images consist of biological, as well as artificially induced correlations resulting from temporal and spatial image reconstruction processes. The ultimate goal of this research is to develop a framework to identify true biological correlations within processed data. Analyzing the operators applied to the data during the reconstruction process facilitates a means of quantifying the effects that spatial reconstruction operators have on specific temporal frequency bands. This essay will outline the process of deriving the exact theoretical statistical relationships for the spatial covariance and spatial correlation matrices as a linear combination of second order voxel temporal frequencies. With an understanding of these matrices, the benefit of developing a matrix notation framework with respect to the application of spatial processing operators will be discussed. The final portion of the essay will provide insight into the next steps of the research that aims to quantify which frequency bands the artificial spatial correlations are induced into.

III. FREQUENCY REPRESENTATION

In MRI the data acquired is Fourier encoded from magnetic field gradients, thus the spatial information measured regarding an object in the scanner is ideally the Fourier transform of the object. The inverse Fourier transform (IFT) is applied to the acquired *k*-space data, resulting in a reconstructed image. If the spatial IFT is represented as the complex-valued matrix, $\Omega_C = \Omega_R + \mathrm{i}\Omega_I$, and complex-valued spatial frequencies are represented in matrix form as $F_C = F_R + iF_I$, then the complex-valued image is represented in the matrix form, $Y_C = \Omega_C F_C \Omega_C^T$ [Rowe, 2007]. This relationship between the image domain and the spatial frequency domain provides a means to represent spatial covariance and spatial correlation matrices in terms of temporal frequencies. By converting the voxel time-series into its constituent temporal frequencies, one can determine the frequency bands that contribute significantly towards the spatial correlation between voxels.

To find the spatial correlation between p voxels over n time repetitions (TRs), define Y as $2n$ real-valued $n_{row} \times n_{col}$ image representations of Y_C, which is n complex-valued $n_{row} \times n_{col}$ images, and y is a vectorized version of Y of length $2pn$ where $p = n_{row}n_{col}$. The vector y is formed by concatenating images that are ordered by row with all real voxel values of an image stacked over all of the corresponding imaginary voxel values. The time-series is then permuted with a permutation matrix, P, such that $v = Py$, and v is $2pn \times 1$ vector ordered by voxel with the real components stacked over the imaginary components for each voxel time-series. The voxel time-series are Fourier transformed into the temporal frequency domain, such

that $f = \left(I_p \otimes \bar{\Omega}_T\right) Py$ is a $2pn \times 1$ vector with the real temporal frequencies of each voxel stacked upon the corresponding imaginary temporal frequencies.

A. Simulation: Impact of Smoothing

As discussed in the introduction, spatial smoothing operators are commonly applied after the image reconstruction process to increase image contrast, $f_S = \left(I_p \otimes \bar{\Omega}_T\right) P(I_n \otimes S_m) y$. While spatial smoothing minimizes the influence of noise in reconstructed images, the application of a spatial smoothing operator, S_m, induces a correlation between a voxel and its neighbors. In a MATLAB Monte Carlo simulation, a time series of 256 images of a 55×55 Shepp-Logan phantom was generated, where each image was smoothed with a Gaussian kernel with a full-width-at-half-maximum (FWHM) of 3 voxels. After computing the voxel correlation matrix, the correlation between a particular voxel (such as the center one) and all other voxels can be represented as an image. As illustrated in Fig. 1a, before smoothing the images, the centrally located voxel appears to have no correlation with the other voxels; however, the post-smoothing image in Fig. 1b reveals the centrally located has a significantly increased spatial correlation with neighboring voxels. Note, in this simulation the degree and the extent the induced correlation extends to neighboring voxels are dependent on the FWHM of the smoothing operator.

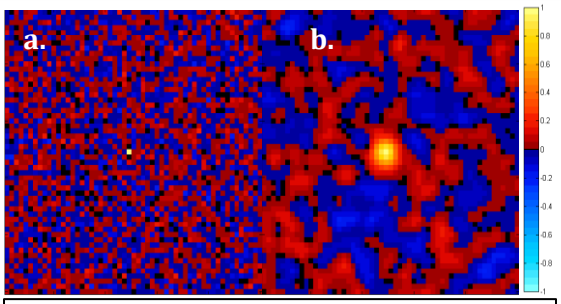

Figure 1. Frequency correlation map between a centrally located voxel and all other voxels: (a) before smoothing (b) after smoothing.

In addition to observing the effects of smoothing on the spatial correlation maps, Fig. 2 demonstrates the impact of the smoothing operator on two neighboring voxel temporal frequency spectrums. Examining how the smoothing operator modifies the temporal frequency spectrums in Fig. 2, first indicates the smoothing operator forces the two temporal frequency spectrums to appear to be more in sync throughout their entire spectrums, and second, Fig. 2b reveals artificially induced peaks in the temporal frequency spectrums as indicated with arrows. Thus, specific temporal frequency bands may induce spatial correlations with greater magnitude when compared to other temporal frequency bands. To further understand the extent of the impact of spatial and temporal processers on functional connectivity, consider three voxel time series, v_a, v_b, and v_c. Assume v_a and v_b are correlated, v_b and v_c are correlated, but v_a and v_c are not correlated. In the following sections, it will be shown that the correlations between v_a and v_b, as well as v_b and v_c, arise from overlapping temporal frequency spectrums. Although v_a and v_c are not correlated because they do not share overlapping temporal frequency spectrums, spatial

preprocessing alters the frequency spectrums of each voxel, such that v_a and v_c now have overlapping frequency content, and thus an induced correlation.

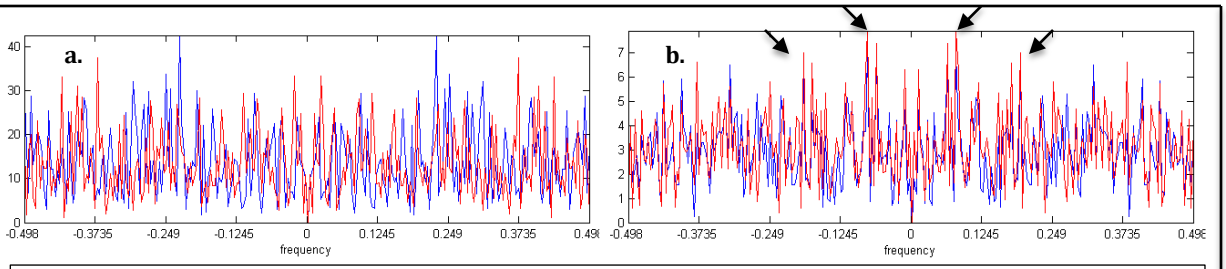

Figure 2. The temporal frequency spectrums for two neighboring voxels: (a) before smoothing (b) after smoothing.

B. The Spatial Covariance Matrix

For the demeaned time series of any two voxels, v_j and v_k, the spatial covariance between the time-series of voxel j and the time-series of voxel k can be represented as $\text{cov}(v_j, v_k) = \frac{1}{n}(v_j)'(v_k)$. Define $\mathbf{E}[v_j] = \mu_j$ and $\mathbf{E}[v_k] = \mu_k$, such that $\mu_j = [\mu_{jR_1} \dots \mu_{jR_n} \mu_{jI_1} \dots \mu_{jI_n}]$ and $\mu_k = [\mu_{kR_1} \dots \mu_{kR_n} \mu_{kI_1} \dots \mu_{kI_n}]$, $\mathbf{var}[v_j] = \sigma^2 I_{2n}$ and $\mathbf{var}[v_k] = \sigma^2 I_{2n}$, and $\Sigma_{j,k}$ is the $2n \times 2n$ temporal covariance matrix for the time-series of voxel j and k that is further defined in the appendix. The expected value for spatial covariance between the time-series of voxel j and the time-series of voxel k is represented as

$$\mathbf{E}[\text{cov}(v_j, v_k)] = \mathbf{E}\left[\frac{1}{n}(v_j)'(v_k)\right] = \frac{1}{n}\sum_{i=1}^{n}\left(\mu_{jR_i}\mu_{mR_i} + \sigma_{jR_i,mR_i} + \mu_{jI_i}\mu_{mI_i} + \sigma_{jI_i,mI_i}\right)$$

$$= \frac{1}{n}\left(\mu_j'\mu_k + tr(\Sigma_{j,k})\right). \quad (1)$$

Using the identities: $\Omega_R\Omega'_R = \frac{n}{2}I_n$, $\Omega_I\Omega'_I = \frac{n}{2}I_n$, and $\Omega_R\Omega'_I = 0$, the spatial covariance between the demeaned time-series of any two voxels, v_j and v_k, can be represented as a summation of second order temporal frequencies by

$$\operatorname{cov}(v_j, v_k) = \frac{1}{n}(v_j)'(v_k) = \frac{1}{n}\left[(\Omega_R f_{jR} - \Omega_I f_{kI})'(\Omega_R f_{jR} - \Omega_I f_{kI})\right]$$

$$= \frac{1}{2}\left[f'_{jR}f_{kR} + f'_{jI}f_{kI}\right] = \frac{1}{2}\sum_{i=1}^{n}\left(f_{jR_i}f_{kR_i} + f_{jI_i}f_{kI_i}\right).$$

To find the expected value for the spatial covariance in terms of temporal frequencies, define $\mathbf{E}[f_j] = \mathbf{E}[\overline{\Omega}_T v_j] = \overline{\Omega}_T\mu_j$ and $\mathbf{E}[f_k] = \overline{\Omega}_T\mu_k$, $\mathbf{cov}[f_j] = \overline{\Omega}_T\sigma^2 I_{2n}\overline{\Omega}'_T = \sigma^2 I_{2n}\overline{\Omega}_T\overline{\Omega}'_T = \frac{\sigma^2}{n}I_{2n}$ and $\mathbf{cov}[f_k] = \frac{\sigma^2}{n}I_{2n}$, and $\overline{\Omega}_T\Sigma_{j,k}\overline{\Omega}'_T$ is the $2n \times 2n$ temporal covariance matrix for voxel j and k frequency spectrums that is further defined in the appendix. Since $\mathbf{E}[\operatorname{cov}(v_j, v_k)] = \mathbf{E}\left[\frac{1}{2}\sum_{i=1}^{2n}\left(f_{j_i}f_{k_i}\right)\right]$ and $\overline{\Omega}_T\overline{\Omega}'_T = \frac{1}{n}$, the expected value for spatial covariance in terms of second order temporal frequencies between the voxel j and voxel k is represented as

$$\mathbf{E}\left[\frac{1}{2}f'_j f_k\right] = \frac{1}{2}\left[(\overline{\Omega}_T\mu_j)'(\overline{\Omega}_T\mu_k) + tr\left(\overline{\Omega}_T\Sigma_{j,k}\overline{\Omega}'_T\right)\right] = \frac{1}{2}\left[\frac{1}{n}\mu'_j\mu_k + tr\left(\overline{\Omega}_T\Sigma_{j,k}\overline{\Omega}'_T\right)\right].$$

Furthermore, the spatial covariance between two voxels in Eq. (1) can be expanded into a $p \times p$ symmetric covariance matrix, Σ_v, for all voxels, such that the *jth* row and *kth* column of Σ_v represents the spatial covariance between the time-series for voxels j and k in terms of temporal frequencies,

$$\Sigma_v = \frac{1}{n}\begin{bmatrix} \sum_{i=1}^{n}\left(v_{1R_i}^2 + v_{1I_i}^2\right) & \cdots & \sum_{i=1}^{n}\left(v_{1R_i}v_{pR_i} + v_{1I_i}v_{pI_i}\right) \\ \vdots & \ddots & \vdots \\ \sum_{i=1}^{n}\left(v_{pR_i}v_{1R_i} + v_{pI_i}v_{1I_i}\right) & \cdots & \sum_{i=1}^{n}\left(v_{pR_i}^2 + v_{pI_i}^2\right) \end{bmatrix}.$$

Represent the voxel time-series in the $p \times 2n$ matrix form as $V = \begin{bmatrix} v'_{1R}\ v'_{1I} \\ v'_{2R}\ v'_{2I} \\ \vdots \\ v'_{pR}\ v'_{pI} \end{bmatrix}$ with $[V] = \begin{bmatrix} \mu'_{1R}\ \mu'_{1I} \\ \mu'_{2R}\ \mu'_{2I} \\ \vdots \\ \mu'_{pR}\ \mu'_{pI} \end{bmatrix}$. Note, V is a $p \times 2n$ matrix with the *jth* row comprised of a vector with the real time-series component for voxel *j* stacked upon the imaginary time-series component for voxel *j*. Then the $p \times p$ spatial covariance matrix for the voxels time-series is constructed as a series of matrix multiplications, $\mathbf{E}[\Sigma_v] = \frac{1}{n}\mathbf{E}[V]\mathbf{E}[V'] + \frac{1}{n}vec(\Sigma_\sigma)\Lambda$ as defined and described below.

Since one can determine the frequency bands that have the greatest contribution towards the spatial correlation between voxels, by converting the voxel time-series into temporal frequencies, the motivation for this section is to represent to the spatial covariance matrix in terms of temporal frequencies

$$\Sigma_f = \frac{1}{2}\begin{bmatrix} \sum_{i=1}^{n}\left(f_{1R_i}^2 + f_{1I_i}^2\right) & \cdots & \sum_{i=1}^{n}\left(f_{1R_i}f_{pR_i} + f_{1I_i}f_{pI_i}\right) \\ \vdots & \ddots & \vdots \\ \sum_{i=1}^{n}\left(f_{pR_i}f_{1R_i} + f_{pI_i}f_{1I_i}\right) & \cdots & \sum_{i=1}^{n}\left(f_{pR_i}^2 + f_{pI_i}^2\right) \end{bmatrix}$$

This matrix is formed through the multiplication, $\Sigma_f = \frac{1}{2}FF'$, where, similar to V, $F = \begin{bmatrix} f'_{1R}\ f'_{1I} \\ f'_{2R}\ f'_{2I} \\ \vdots \\ f'_{pR}\ f'_{pI} \end{bmatrix}$, then the expected value for this $p \times p$ spatial covariance matrix is represented as $\mathbf{E}\left[\Sigma_f\right] = \frac{1}{2n}\mathbf{E}[V]\mathbf{E}[V'] + \frac{1}{2}vec(\Sigma_{\Omega\sigma})\Lambda$.

Note, the Λ matrix is a $4pn^2 \times p$ matrix of 1's and 0's, and the $p \times 4n^2p$ matrices $\text{vec}(\Sigma_\sigma)$ and $\text{vec}(\Sigma_{\Omega\sigma})$ are composed of temporal covariances, and are further

described in the appendix. The element representation of the covariance and correlations of the spatial covariance matrix are also presented in the appendix.

C. The Spatial Correlation Matrix

For the demeaned time series of any two voxels, v_j and v_k, the spatial covariance between voxels *j* and *k* can be represented as a summation of second order temporal frequencies by

$$\operatorname{corr}(v_j, v_k) = \frac{\operatorname{cov}(v_j, v_k)}{\sqrt{\operatorname{var}(v_j)\operatorname{var}(v_k)}} = \frac{\sum_{i=1}^{n}\left(f_{jR_i}f_{kR_i}+f_{jI_i}f_{kI_i}\right)}{\sqrt{\sum_{i=1}^{n}\left(f_{jR_i}f_{jR_i}+f_{jI_i}f_{jI_i}\right)\sum_{i=1}^{n}\left(f_{kR_i}f_{kR_i}+f_{kI_i}f_{kI_i}\right)}}.$$

Also, by using the derivations from the previous section, the expected value of the spatial covariance matrix is represented as a summation of second order temporal frequencies by

$$\mathbf{E}\left[\,\Sigma_f\right] = \frac{1}{2}\begin{bmatrix} \frac{1}{n}\mu_1'\mu_1 + tr(\overline{\Omega}_T\Sigma_1\overline{\Omega}_T') & \cdots & \frac{1}{n}\mu_1'\mu_p + tr\left(\overline{\Omega}_T\Sigma_{1,p}\overline{\Omega}_T'\right) \\ \vdots & \ddots & \vdots \\ \frac{1}{n}\mu_p'\mu_1 + tr\left(\overline{\Omega}_T\Sigma_{p,1}\overline{\Omega}_T'\right) & \cdots & \frac{1}{n}\mu_p'\mu_p + tr\left(\overline{\Omega}_T\Sigma_p\overline{\Omega}_T'\right) \end{bmatrix}.$$

Define $D_{\Sigma f}$ as a diagonal matrix consisting of the diagonal elements of $\mathbf{E}\left[\,\Sigma_f\right]$, a $p \times p$ matrix with only the expected value of the spatial variances on the diagonal. A symmetric $p \times p$ spatial correlation matrix constructed from the expected value of the spatial covariance matrix is formed with the multiplication

$$R_{\Sigma f} = D_{\Sigma f}^{-1/2}\mathbf{E}\left[\,\Sigma_f\right]D_{\Sigma f}^{-1/2},$$

where the *jth* row and *kth* column of $R_{\Sigma f}$ is the spatial correlation between voxels *j* and *k*.

D. Processing Operator Application

Representing the spatial covariance and correlation in matrix form, constructed from a series of matrix multiplications allows one to measure the effect of the temporal and spatial processing operators. For example, as described in a previous section, the smoothed temporal frequencies are constructed with the multiplication $f_S = \left(I_p \otimes \bar{\Omega}_T\right) P (I_n \otimes S_m) y$. If the $2pn \times 2pn$ spatiotemporal covariance matrix for the $2pn \times 1$ real-valued time-series y is Γ, $\mathbf{E}[y] = \mu$, and $O = \left(I_p \otimes \bar{\Omega}_T\right) P (I_n \otimes S_m)$, which is the order of operations applied to the time-series, then $\mathbf{E}[f_S] = O\mu$ and $\mathbf{cov}[f_S] = O\Gamma O'$. Developing a standard framework, such that changes in the structure of the spatial covariance matrix or spatial correlation matrix are observed when a spatial or temporal operator is applied to the data, provides a means to quantify to the processing operators, and reveal the true spatiotemporal correlations.

IV. FUTURE RESEARCH

Representing these statistical relationships in terms of their constituent temporal frequencies provides a framework for identifying the frequency bands that contribute substantially to the induced correlations as a result of image reconstruction and processing operations. If the temporal frequency bands that induce a spatial correlation are identified, potentially a method can be developed to regress or filter out the correlation inducing frequency bands such that the true spatiotemporal correlation is revealed. Thus, the next steps of this research are to decompose the temporal frequency spectrums, to determine which temporal frequency bands contribute significantly to the induced correlations between voxel regions of interest, and to measure the magnitude of which the temporal frequency bands contribute to the induced correlation. Furthermore, the statistical derivations of the true values for the spatial covariance and correlation matrices will be tested on experimental data.

V. CONCLUSION

To correct the noise inherent within the signal and identify the true biological spatiotemporal correlations, spatial and temporal filters are applied during the time series data processing. Although, it is well known that spatial preprocessing induces correlation between voxels. Deriving the exact spatial covariance and correlation matrices in terms of each voxel's constituent temporal frequencies, provides a framework to measure the impact of applying any individual spatial and temporal operator or series of spatial and temporal operators. The next step of this research is to quantify the magnitude that specific frequency bands create artificial correlations within the data, and develop a means to regress or filter out the induced spatial correlations, such that the processed data will yield increased diagnostic evaluations in human clinical fMRI evaluations.

APPENDIX

The p x $4pn^2$ matrices, $vec(\Sigma_\sigma) = \begin{bmatrix} \mathrm{vec}(\Sigma_{1,1}) & \cdots & \mathrm{vec}(\Sigma_{1,\mathrm{p}}) \\ \vdots & \ddots & \vdots \\ \mathrm{vec}(\Sigma_{\mathrm{p},1}) & \cdots & \mathrm{vec}(\Sigma_{\mathrm{p,p}}) \end{bmatrix}$

and $vec(\Sigma_{\Omega\sigma}) = \begin{bmatrix} \mathrm{vec}(\overline{\Omega}_T \Sigma_{1,1} \overline{\Omega}'_T) & \cdots & \mathrm{vec}(\overline{\Omega}_T \Sigma_{1,\mathrm{p}} \overline{\Omega}'_T) \\ \vdots & \ddots & \vdots \\ \mathrm{vec}(\overline{\Omega}_T \Sigma_{\mathrm{p},1} \overline{\Omega}'_T) & \cdots & \mathrm{vec}(\overline{\Omega}_T \Sigma_{\mathrm{p,p}} \overline{\Omega}'_T) \end{bmatrix}$,

are constructed from the symmetric $2pn$ x $2pn$ Σ_σ matrix, $\Sigma_\sigma = \begin{bmatrix} \Sigma_{1,1} & \cdots & \Sigma_{1,p} \\ \vdots & \ddots & \vdots \\ \Sigma_{p,1} & \cdots & \Sigma_{p,p} \end{bmatrix}$,

comprised of the symmetric $2n$ x $2n$ $\Sigma_{j,k}$ matrices,

$$\Sigma_{j,k} = \begin{bmatrix} \sigma_{jR_1,kR_1} & \cdots & \sigma_{jR_1,kR_n} & \sigma_{jR_1,kI_1} & \cdots & \sigma_{jR_1,kI_n} \\ \vdots & \ddots & \vdots & \vdots & \ddots & \vdots \\ \sigma_{jR_n,kR_1} & \cdots & \sigma_{jR_n,kR_n} & \sigma_{jR_n,kI_1} & \cdots & \sigma_{jR_n,kI_n} \\ \sigma_{jI_1,kR_1} & \cdots & \sigma_{jI_1,kR_n} & \sigma_{jI_1,kI_1} & \cdots & \sigma_{jI_1,kI_n} \\ \vdots & \ddots & \vdots & \vdots & \ddots & \vdots \\ \sigma_{jI_n,kR_1} & \cdots & \sigma_{jI_n,kR_n} & \sigma_{jI_n,kI_1} & \cdots & \sigma_{jI_n,kI_n} \end{bmatrix}.$$

BIBLIOGRAPHY

Biswal, B., Yetkin, F.Z., Haughton, V.M., Hyde, J.S. Functional Connectivity in the Motor Cortex of Resting Human Brain Using Echo-Planar MRI. Magn. Reson. Med. 1995; 34:537-541.

Bohanna, I., Georgiou-Karistianis,N., Hannan, A.J., Egan, G.F. Magnetic resonance imaging as an approach towards identifying neuropathological biomarkers for Huntington's disease. Brain Research Reviews 2008; 58,209-225.

Bruce, I.P., Karaman, M. M, Rowe, D.B. A Statistical Examination of the SENSE Reconstruction via an Isomorphism Representation. Magn. Reson. Imag. 2011;29, 1267-1287.

Davey, C.E., Grayden, D.B., Egan, G.F., Johnston, L.A., Filtering induces correlation in fMRI resting state data. NeuroImage 2013; 64, 728-740.

Fox, M.D., Greicius M. Clinical applications of resting state functional connectivity. Frontiers in Systems Neuroscience 2010; 4(19) .

Kleinhans, N.M.,Richards, T., Sterling, L., Stegbauer, K.C., Mahurin, R., Johnson, L.C., Greenson J., Dawson, G., Aylward, E. Abnormal functional connectivity in autism spectrum disorders during face processing. Brain 2008;131 (4): 1000-1012.

Li, S., Li, Z., Wu, G., Zhang, M., Franczak, M., Antuono, P.G. Alzheimer Disease: Evaluation of a Functional MR Imaging Index as a Marker. Radiology 2002; 225: 253-259.

Lowe, M. J., Mock, B.J., Sorenson, J. A. Functional Connectivity in Single and Multislice Echoplanar Imaging Using Resting-State Fluctuations. Neuroimage 1998; 7: 119–132.

Nencka, A.S., Hahn, A.D., Rowe, D.B. A Mathematical Model for Understanding Statistical Effects of k-space (AMMUST-k) Preprocessing on Observed Voxel Measurements in fcMRI and fMRI. J. Neurosci. Meth. 2009;181, 268–282.

Ogawa, S., Lee, T.M., Kay, A.R., Tank, D.W. Brain Magnetic Resonance Imaging with Contrast Dependent on Blood Oxygenation. Proc. Natl. Acad. Sci. USA 1990; 87: 9868-9872.

Rowe DB, Nencka AS, Hoffmann RG. Signal and noise of Fourier reconstructed fMRI data. J.of Neurosci. Meth. 2007; 159:361–369.

Marquette University

This is to certify that we have examined this copy of the thesis by

Mary C. Kociuba

and have found that it is complete and satisfactory in all respects.

This thesis has been approved by:

_____

Dr. Daniel B. Rowe
Department of Mathematics, Statistics, and Computer Science

Approved on

_____